博士論文

THE EFFECTS OF SYNDECAN ON OSTEOBLASTIC CELL ADHESION ONTO NANO-ZIRCONIA SURFACE

SUN Lu

A Dissertation Submitted For Degree Of Doctor Of Philosophy
Department of Advanced Prosthetic Dentistry
Graduate School of Dentistry
Tohoku University
2020

Abstract

Purpose: Zirconia is one of the most promising implant materials due to its favorable physical, mechanical and biological properties. However, until now, we know little about the mechanism of osseointegration on zirconia. The purpose of this study is to evaluate the effect of Syndecan (Sdc) on osteoblastic cell (MC3T3-E1) adhesion and proliferation onto zirconia materials.

Materials and methods: The mirror-polished disks 15 mm in diameter and 1.5 mm in thick of commercial pure titanium (CpTi), 3mol% yttria-stabilized tetragonal zirconia polycrystalline (3Y-TZP) and Nano-Zirconia (NanoZr) are used in this study. MC3T3-E1 cells were seeded onto specimen surfaces and subjected to RNA interference (RNAi) for Syndecan-1, Syndecan-2, Syndecan-3, and Syndecan-4. At 48h post-transfection, the cell morphology, actin cytoskeleton, and focal adhesion were observed using scanning electron microscopy or laser scanning confocal fluorescence microscopy. At 24h and 48h post-transfection, cell counting kit-8 (CCK-8) assay was used to investigate the cell proliferation.

Results: The cell morphology of MC3T3-E1 cells on CpTi, 3Y-TZP, and NanoZr changed into abnormal shape after gene silencing of Syndecan. Among the Syndecan family, Sdc-2 is responsible for NanoZr specific morphology regulation, via maintenance of cytoskeletal conformation without affecting cellular attachment. According to CCK-8 assay, Sdc-2 affects the osteoblastic cell proliferation onto NanoZr.

Conclusion: Within the limitation of this study, we suggest that Syndecan affect osteoblastic cell adhesion on CpTi, 3Y-TZP, and NanoZr. Sdc-2 is an important Heparin-sensitive cell membrane regulator in osteoblastic cell adhesion, specifically on NanoZr, through the organization of actin cytoskeleton and affects osteoblastic cell proliferation.

Keywords: Syndecan, Zirconia, Cell Adhesion, Osteoblastic Cell

List of Tables and Figures

Chapter 1. INTRODUCTION

Ceramic dental implants attract attention from the view of metal-free and aesthetic dentistry, due to their non-allergic reactions, non-metal deposition, and non-tissue discoloration.[1-3] The first ceramic dental implant system made of aluminum oxide (Al_2O_3) is not recommended for making dental implants, due to its fragility caused by high hardness and elastic modulus. [4,5]

In recent years, zirconia ceramics are the most promising candidate as a dental implant material, relying on its good mechanical properties, stable physical and biological properties, outstanding biocompatibility, as well as its nature-tooth-like color. Additionally, zirconia-oxide (ZrO_2) surfaces showed a significant reduction of the presence of bacteria than titanium surfaces, which can protect implants from peri-implantitis.[6,7] The 3mol% yttria-stabilized tetragonal zirconia polycrystalline (3Y-TZP) which is primarily used as dental zirconia has solid mechanical properties, [8,9] however, it also has a high risk of fracture than titanium implant.[10–12] Therefore, Nano-Zirconia (NanoZr), a ceria-stabilized nanocomposite (10mol% CeO2-ZrO2 and 30vol% Al2O3) [13] , not only had superior fracture strength and fracture toughness but also showed excellent mechanical durability for LTD (low-temperature degradation) compared with 3Y-TZP, [14,15] suggesting as a potential alternative to titanium in dental implant. Furthermore, we recently reported that NanoZr has good biocompatibility due to adhesion-dependent osseointegration, however, precise molecular mechanism and key regulator gene(s) are remain unclear.

The adhesion of anchorage-dependent osteoblast cells is a critical procedure for subsequent cell functions and activities pertinent to new bone formation.[16] Cell adhesion is the result of a cell-extracellular matrix (ECM) - biomaterial binding, composed of two different phenomena. The first phase is called the attachment phase, which occurs quickly using physical and chemical factors, such as hydrogen bond, ionic forces and van der Walls forces. The second phase lasts in a long period involving numerous proteins, including ECM proteins, cytoskeleton proteins, and cell membrane proteins.[17,18]

Cell membrane protein also works as a membrane receptor, primarily mediates cell adhesion to ECM proteins. It has been widely known that integrin is the main cell surface adhesion receptor which can detect the exposure of the Arg-Gly-Asp (RGD) motif of ECM proteins specifically. The results of competitive inhibition test using synthetic RGD peptides showed that RGD peptides remarkably inhibited the adhesion of osteoblast on hydroxyapatite but not on titanium.[19] In our previous study, we found that initial osteoblast adhesion onto the zirconia surface is regulated by integrins and heparin-sensitive molecules.[20] Consistently, some studies even indicated that the binding to integrin receptor alone is not enough to promote cell adhesion without the participation of heparan sulfate proteoglycans (HSPGs).[21,22]

The major type of transmembrane HSPG species of cells is the Syndecan family.[23] Recent studies showed that Syndecan is considered to be a co-receptor with integrin in cell adhesion.[24] There are four members of the Syndecan family in mammals, consists of

Syndecan-1 (Sdc-1), Syndecan-2 (Sdc-2), Syndecan-3 (Sdc-3) and Syndecan-4 (Sdc-4). It is reported that Sdc-2 and Sdc-4 is required for generating signals for the assembly of focal adhesions.[25–27] However, the detail role of each Syndecan family is not studied especially in cell adhesion including osteoblasts.

This study aims to elucidate the role of Syndecan family in osteoblast adhesion onto the zirconia surface. The dental implant biomaterials in the next generation must be designed for supporting osteoblast adhesion. In this study, we use osteoblast-like cell line MC3T3-E1 to investigate the effect of the Syndecan family in cell adhesion onto the zirconia surface.

Chapter 2. MATERIALS AND METHODS

2.1 Specimen preparation

The disks 15mm in diameter and 1.5mm in thick of commercial pure titanium (CpTi, Nippon Steel Co. Japan), 3Y-TZP (Yamamoto Precious Metal Co. Japan), and NanoZr (Yamamoto Precious Metal Co. Japan) were used in this study. Each surface of the specimens was mirror-polished with aluminum oxide waterproof abrasive paper (200#, 400#, 600#, 800#). Then the disks were cleaned by sonication with acetone, ethanol, and deionized distilled water. After that, the specimens were treated under UV light lasted 30 minutes for each side by using a 15W bactericidal lamp (Toshiba, Tokyo, Japan), followed by immersion in 75% ethanol for 10 minutes and ultrapure water for 3 minutes. Finally, the specimens were stored in an airtight container for further use.

2.2 Cell culture

MC3T3-E1 cells, osteoblast-like cells from rat calvaria were obtained (ATCC CRL-2594) and cultured in a sterile cell culture dish with alpha-modified minimum essential medium (α-MEM, Nacalai tesque, Kyoto, Japan) supplemented with 10% FBS (fetal bovine serum, Gibco Life Technologies Inc., Grans Island, NY, USA) and 1% penicillin-streptomycin (Gibco Life Technologies Inc.). Cells were cultured at 37°C, 5% CO2, 95% humidity, and passaged at 80% confluence by using 0.25% Trypsin-EDTA (Gibco Life Technologies Inc.).

2.3 RNA interference

Stealth siRNAs for mouse Syndecan-1 (Catalog No. #1, MSS209928; #2, MSS209929), Syndecan-2 (Catalog No. #1, MSS236834; #2, MSS236835), Syndecan-3 (Catalog No. #1, MSS238079; #2, MSS238080), Syndecan-4 (Catalog No. #1, MSS238085; #2, MSS238086), and Stealth RNAi Negative Control was purchased from Invitrogen. MC3T3-E1 cells were seeded at a density of 5×10^3 cells/well or 5×10^4 cells/well onto CpTi, 3Y-TZP, and NanoZr, then transfected with 40 pmol/well of indicated siRNA or Negative Control siRNA using Lipofectamine RNAiMAX (Invitrogen, UK). A 24-well-plate (Plate, Thermo Fisher Scientific) without specimens was taken to be a control group. After 48 hours of transfection, the efficiency of RNA interference (RNAi) was detected by quantitative RT-PCR analysis.

2.4 Quantitative RT-PCR analysis

Total RNA was extracted from osteoblast-like cells by using SingleShot Cell Lysis Kit (Bio-Rad Laboratories, Inc. Hercules, CA, USA), and the cDNAs were synthesized using iScriptTM Advanced cDNA Synthesis Kit (Bio-Rad Laboratories, Inc. Hercules, CA, USA) following the manufacture's protocol. Quantitative RT-PCR analysis was then performed with CFX96TM Real-Time PCR Detection System (Bio-Rad, USA) using SsoAdvacnedTM Universal SYBR® Green Supermix (Bio-Rad, USA). The sequences of PCR primers were listed in Table 1. Relative gene expression was calculated compared with the expression of GAPDH mRNA by

using comparative CT (ΔΔCT) relative quantification method of qRT-PCR.

2.5 Cell morphology analysis

After RNA interference and incubation for 48 hours, the cells (5×10^3 cells/well) were fixed with 2.5% glutaraldehyde (Wako Pure Chemical Industries) for 30 minutes. Then dehydrated at a graded concentration of ethanol (15 minutes once at 50%, 60%, 70%, 80%, 90%, 95%; 2 minutes twice at 100%) and dried. After sputter coating with gold-palladium, the surfaces were observed with accelerating voltage of 15kV and 100×, and 1,000× magnification by scanning electron microscopy (SEM, JSM-6390LA, JEOL Ltd, Tokyo, Japan).

To investigate the actin cytoskeleton, the cells (5×10^3 cells/well) were fixed with 4% paraformaldehyde (Wako Pure Chemical Industries) for 30 minutes at room temperature, rinsed with PBS, permeabilized with 0.2% (v/v) Triton X-100 and blocked using 1% BSA (Bovine Serum Albumin, Sigma Aldrich Co., St Louis, MO, USA) for 30 minutes. The cells were then stained with Rhodamine-Phalloidin (Cytoskeleton Inc., Denver, Co, USA) for 30 minutes at room temperature, followed by rinses with PBS, finally stained with DAPI Fluoromount-G (DAPI, Southern Biotech Co., Birmingham, AL, USA) for 5 minutes. The cell cytoskeleton and nucleus were observed by laser scanning confocal fluorescence microscopy (LSCM, TCS SP8, Leica Microsystem Co., Tokyo, Japan). The cell spread area ratio was traced in all samples, the

ratio of cell spread area between si-Sdc group and si-NegCont group was integrated using an image analysis software (ImageJ, National Institutes of Health, USA).

For immunostaining of vinculin protein, cells (5×10^3 cells/well) were first incubated with rabbit-anti-mouse vinculin monoclonal antibody overnight and then treated by a goat-anti-rabbit secondary antibody (Invitrogen, Thermo Fisher Scientific, MA, USA). Finally, samples were observed using LSCM.

2.6 Cell proliferation analysis

After 24h and 48h post-transfection of Syndecan, the cell counting kit (CCK-8, Dojindo, Kumamoto, Japan) reagent (50μL) was added into each well diluted by 500μL α-MEM medium and incubated for 1 hour. A blank control well containing only CCK-8 reagent and α-MEM medium was set. Subsequently, 100μL of the reaction solution was transferred into a 96-well-plate in triplicate. The optical density was measured with a microplate reader (Bio-Rad iMark Microplate Reader, Hercules, CA, USA) at a wavelength of 450nm.

2.7 Statistical analysis

All of the experiments were repeated at least three times using independent sample. Statistical analysis was performed using one-way ANOVA followed by the Student-Newman-Keuls (SNK) multiple comparison test. The significant level was set at 0.05.

Chapter 3. RESULTS

3.1 Quantitative RT-PCR

The results of the qRT-PCR analysis (Figure 1A) showed that Syndecan-1 was attenuated than that of the Negative Control group ($P<0.05$) by both #1 and #2 RNA interference. The knockdown effect is occurred specifically against Sdc-1 without affecting other Syndecans, indicating that off-targeting effects was not observed among Syndecan family members. Significantly increased expression in response to knockdown of other gene were observed in some samples. The transfection efficiency remained consistently on four kinds of materials (Figure 1B-D). Similar results were obtained in all other members of the Syndecan family (Sdc-2, Sdc-3, and Sdc-4). These results suggested that RNA interference was successfully performed among Syndecan family members. The result also indicated that the all Syndecan family members are widely expressed in MC3T3-E1 cells.

3.2 Cell morphology and cell adhesion

Cell morphology and actin cytoskeleton of 48h post-transfection were showed by SEM and LSCM (Figure 2 and Figure 3). As described above, we screened target genes whether both RNAi for #1 and #2 shows same reaction or not. Cell morphology of MC3T3-E1 cells tended to be irregularly triangular and thinner than the Negative Control group on different surfaces. On the NanoZr surface, the cells were small and spherical after Syndecan-2 knockdown.

Moreover, the osteoblastic cells appeared more micro-filaments than the Negative Control group on each surface, and these long-spreading micro-filaments built more communication branches on cell-to-cell contacts. After staining vinculin protein, we found that vinculin existed in every transfected group (Figure 4). These changes in cell morphology seem to be more obvious on zirconia and titanium in comparison to the plate. Additionally, after the RNA interference of Syndecan, the focal adhesion was not impaired.

3.3 Cell proliferation

As Figure 5A shows, on the surface of NanoZr, the absorbance value of cells in si-Sdc2 (#1, #2) group showed significantly lower than the Negative Control group after 24h transfected (P<0.05). The absorbance values between the Negative Control group and transfected groups showed no significant difference on the surface of CpTi, 3Y-TZP, or Plate. Similarly, at 48h time point, the absorbance value of cells in si-Sdc2 (#1, #2) group on NanoZr showed significantly lower than the Negative Control group (Figure 5B). Meanwhile, compared with two time points, the absorbance value of cells increases on every material. It suggests that the MC3T3-E1 cells still growing on all the surfaces from 24h to 48h even after Syndecan gene silencing.

Chapter 4. DISCUSSION

Zirconia dental implant has great advantages in metal-free dentistry and esthetic dentistry. 3Y-TZP, a form of zirconia-oxide, is widely used in dentistry as prosthetic devices decades ago. In 1985, Tsukuma [28,29] reported that ceria-stabilized tetragonal zirconia (Ce-TZP) shows a high toughness and a complete resistance to LTD in comparison to those of Y-TZP.[30] In 1998, a Ce-TZP based nanostructured composite (NanoZr) was developed.[31] As an oxide ceramic material, zirconia dental implant treatment can provide an aesthetic outcome in patients relying on its satisfactory color and excellent biocompatibility.

Osteoblasts are anchorage-dependent cells, and the attachment of osteoblasts to the substrate material is the physiological basis for cell proliferation, cell migration, and cell differentiation.[32] To evaluate the biocompatibility or biological activity of dental implant material, the prerequisite point is its ability to actively induce osteoblasts to attach to the material surface.[33] However, the mechanism of osteoblast cell adhesion onto zirconia is still incompletely understood. In the presented study, we try to investigate the molecular mechanism of osteoblast-like cell adhesion onto the zirconia surface.

In response to interaction signals, osteoblast changes both cell shape and cell adhesion to material surfaces, which determined by rearrangements of the actin cytoskeleton.[34] After silencing Syndecans, osteoblast changes both its shape and adhesion state (Figure 3). MC3T3-E1 cells can’t spread completely on CpTi, 3Y-TZP, and NanoZr with low expression of

Syndecan 1-4. Osteoblasts became irregularly triangular or elongated in shape with the formation of filopodia (Figure 3C). Markedly, osteoblasts on the NanoZr surface after transfected with Syndecan-2 showed loss of its normal spindle shape and cell polarity (Figure 3D). It suggests that Syndecan-2 is responsible for NanoZr specific morphology regulator. Syndecans 1–4 are a family of transmembrane proteins composed of a core protein and glycosaminoglycan chains. Although the four syndecans have common functions, they have different tissue distributions and appear to be connected to different signaling pathways. Syndecan-2 is the most abundant syndecan of mesenchymal cell types. In contrast to other syndecans, syndecan-2 expression increases during osteoblast differentiation. Mechanistically, syndecan-2 exerts multiple functions in cells of the osteoblast lineage as it serves as a co-receptor for fibroblast growth factors and Wnt proteins and controls cell adhesion, proliferation, differentiation and apoptosis.[35] Moreover, the chemical composition of NanoZr is different from the CpTi and 3Y-TZP, as well as its physical properties, such as, surface energy or micro current. These might be the possible reasons of syndecan-2 specifically regulates the osteoblastic cell adhesion on NanoZr.

Interestingly, the vinculin staining results showed that the focal adhesion still exists under the condition of Syndecan knockdown (Figure 4). Vinculin is known as an important marker of focal adhesion.[36] therefore MC3T3-E1 cells can still organize focal adhesion under the low expression of Syndecan, but the living condition was impaired. These results suggest that

cellular membrane interface Syndecan-2-mediated cytoskeletal conformation regulates signal transduction of cell viability from zirconia surface.

Generally, F-actin preforms in three forms: when assembled in long bundles, it becomes finger-like protrusions of the plasma membrane called filopodia; when assembled as a meshwork, it becomes sheet-like protrusion known as ruffles or lamellipodia; when arranged in bundles contacting with attachment plaques, actin stress fibers exert force against the substratum.[37] According to the LSCM results, osteoblastic cells showed more filopodia but few lamellipodia after the RNA interference of Syndecan. The filopodia owned longer protrusions, it might be a possible reason for increasing communicating branches between cell-to-cell contacts. Based on the above results, Syndecan-2 may play a role in cell adhesion by affecting the organization of actin cytoskeleton, and by controlling the formation of lamellipodia through a Heparin-dependent mechanism on NanoZr.

According to the cell proliferation results from 24h to 48h culturing, the absorbance values continued growing on the CpTi, 3Y-TZP, NanoZr, and Plate. The absorbance values of cells on CpTi is higher than that on NanoZr, it has been reported that in a long-term animal experiment, the zirconia implants could osseointegrate to the same extent as titanium implants.[38] Intriguingly, at times point 24h and 48h, the absorbance value of MC3T3-E1 cells in si-Sdc-2 (#1, #2) groups showed significantly lower than the Negative Control group ($P<0.05$) on NanoZr. It shows that Syndecan-2 affects the cell proliferation of MC3T3-E1 on NanoZr. It

is notable that Syndecan affects cell morphology on CpTi and 3Y-TZP, but little on cell proliferation. Based on these results, we suppose that Syndecan-2, a Heparin-sensitive protein, specifically affects cell proliferation of osteoblasts via cell morphology regulation on NanoZr. Further, these results suggest that Syndecan-2 mediates mechanobiological regulation of osteoblast integrity on NanoZr.

From qPCR results, we observed when silencing Syndecan-2, the expression level of Syndecan-4 increased. Similarly, silencing of Sdc-1 and Sdc-4 increased Sdc-2 expression on NanoZr (Figure 1D). However, cell morphology or cytoskeleton, and proliferation on NanoZr were not affected in the same condition (Figure 3D, 5A, 5B), suggesting that the basal expression level of Sdc-2 is necessary and sufficient for the maintenance of Syndecan-2 function in our experimental model. This suggests that overexpression of wild-type Sdc-2 may not work as gain-of-function phenotype. Based on protein sequence homology, Syndecan-2 and Syndecan-4 are from one subfamily. Consistent with our results, it has been reported that Syndecan-2 might be regulating its close family member, Syndecan-4.[39] This raise the possibility that increased expression of Syndecan-4 (in the absence of Syndecan-2) modifies cellular activity. However, it is often the case that a silencing of some gene affects expression of other gene(s) in various mechanism even in same gene family.[40,41] The ideal situation is single-knockdown of Syndecan-2, from this point of view, it might be a limitation of this experiment.

In the future study, the examination of the relationship between Syndecan and Integrin on cell adhesion onto the NanoZr surface, as well as the Heparin-related signaling pathway on cell adhesion is needed to be investigated.

Chapter 5. CONCLUSION

Within the limitation of this study, the results suggested that Syndecan1- 4 can be expressed on osteoblastic cells and affects the cell adhesion on CpTi, 3Y-TZP, and NanoZr in varying degrees. Syndecans may play a role in cell morphology and cell adhesion by re-organization the actin cytoskeleton, and possibly by transferring signals from cell to material surface in a Heparin-dependent mechanism. Syndecan-2 may affect the osteoblastic cell adhesion more remarkable on NanoZr, it could also partially regulate osteoblastic cell proliferation.

References

[1]. Sicilia A, Cuesta S, Coma G, et al. Titanium allergy in dental implant patients: A clinical study on 1500 consecutive patients. Clin Oral Implants Res. 2008, 19(8): 823-835.

[2]. Bianco PD, Ducheyne P, Cuckler JM. Local accumulation of titanium released from a titanium implant in the absence of wear. J Biomed Mater Res. 1996, 31(2): 227-234.

[3]. Jung RE, Sailer I, Hämmerle CHF, et al. In vitro color changes of soft tissues caused by restorative materials. Int J Periodontics Restorative Dent. 2007, 27(3): 251.

[4]. Lawson NC, Burgess JO. Dental ceramics: a current review. Compend Contin Educ Dent. 2014, 35(3): 161-166.

[5]. Berge TI, Grønningsaeter AG. Survival of single crystal sapphire implants supporting mandibular overdentures. Clin Oral Implants Res. 2000, 11(2): 154-162.

[6]. Scarano A, Piattelli M, Caputi S, et al. Bacterial Adhesion on Commercially Pure Titanium and Zirconium Oxide Disks: An In Vivo Human Study. J Periodontol. 2004, 75(2): 292-296.

[7]. Nascimento Do C, Pita MS, Fernandes FHNC, et al. Bacterial adhesion on the titanium and zirconia abutment surfaces. Clin Oral Implants Res. 2014, 25(3): 337-343.

[8]. Piconi C, Maccauro G. Zirconia as a ceramic biomaterial. Biomaterials. 1999, 20(1): 1-25.

[9]. Hisbergues M, Vendeville S, Vendeville P. Review zirconia: Established facts and perspectives for a biomaterial in dental implantology. J Biomed Mater Res - Part B Appl

Biomater. 2009, 88(2): 519-529.

[10]. Han JM, Hong G, Lin H, et al. Biomechanical and histological evaluation of the osseointegration capacity of two types of zirconia implant. Int J Nanomedicine. 2016, 11: 6507.

[11]. Gahlert M, Burtscher D, Grunert I, et al. Failure analysis of fractured dental zirconia implants. Clin Oral Implants Res. 2012, 23(3): 287-293.

[12]. Lange FF, Dunlop GL, Davis BI. Degradation During Aging of Transformation-Toughened ZrO2-Y2O3 Materials at 250°C. J Am Ceram Soc. 1986, 69(3): 237-240.

[13]. Sato H, Yamada K, Pezzotti G, et al. Mechanical properties of dental zirconia ceramics changed with sandblasting and heat treatment. Dent Mater J. 2008, 27(3): 408-414.

[14]. Yamashita D, Machigashira M, Miyamoto M, et al. Effect of surface roughness on initial responses of osteoblast-like cells on two types of zirconia. Dent Mater J. 2009, 28(4): 461-470.

[15]. Benzaid R, Chevalier J, Saâdaoui M, et al. Fracture toughness, strength and slow crack growth in a ceria stabilized zirconia-alumina nanocomposite for medical applications. Biomaterials. 2008, 29(27): 3636-3641.

[16]. Hasenbein ME, Andersen TT, Bizios R. Micropatterned surfaces modified with select peptides promote exclusive interactions with osteoblasts. Biomaterials. 2002, 23(19): 3937-3942.

[17]. Anselme K. Osteoblast adhesion on biomaterials. Biomaterials. 2000, 21(7): 667-681.

[18]. Anselme K, Bigerelle M, Noel B, et al. Qualitative and quantitative study of human osteoblast adhesion on materials with various surface roughnesses. J Biomed Mater Res. 2000, 49(2): 155-166.

[19]. Okamoto K, Matsuura T, Hosokawa R, et al. RGD peptides regulate the specific adhesion scheme of osteoblasts to hydroxyapatite but not to titanium. J Dent Res. 1998, 77(3): 481-487.

[20]. Luo F, Hong G, Matsui H, et al. Initial osteoblast adhesion and subsequent differentiation on zirconia surfaces are regulated by integrins and heparin-sensitive molecule. Int J Nanomedicine. 2018, 13: 7657.

[21]. Sim B, Cladera J, O'Shea P. Fibronectin interactions with osteoblasts: Identification of a non-integrin-mediated binding mechanism using a real-time fluorescence binding assay. J Biomed Mater Res - Part A. 2004, 68(2): 352-359.

[22]. Lim CC, Multhaupt HAB, Couchman JR. Cell surface heparan sulfate proteoglycans control adhesion and invasion of breast carcinoma cells. Mol Cancer. 2015, 14(1): 15.

[23]. Woods A, Couchman JR. Syndecan 4 heparan sulfate proteoglycan is a selectively enriched and widespread focal adhesion component. Mol Biol Cell. 1994, 5(2): 183-192.

[24]. Hozumi K, Kobayashi K, Katagiri F, et al. Syndecan- and integrin-binding peptides synergistically accelerate cell adhesion. FEBS Lett. 2010, 584(15): 3381-3385.

[25]. Saoncella S, Echtermeyer F, Denhez F, et al. Syndecan-4 signals cooperatively with integrins in a Rho-dependent manner in the assembly of focal adhesions and actin stress fibers. P Natl Acad Sci USA. 1999, 96(6): 2805-2810.

[26]. Woods A, Couchman JR. Syndecan-4 and focal adhesion function. Curr Opin Cell Biol. 2001, 13(5): 578-583.

[27]. Couchman JR, Woods A. Syndecan-4 and integrins: Combinatorial signaling in cell adhesion. J Cell Sci. 1999, 112(20): 3415-3420.

[28]. Tsukuma K, Shimada M. Strength, fracture toughness and Vickers hardness of CeO2-stabilized tetragonal ZrO2 polycrystals (Ce-TZP). J Mater Sci. 1985, 20(4): 1178-1184.

[29]. Tsukuma K. Mechanical properties and thermal stability of CeO/sub 2/containing tetragonal zirconia polycrystals. Am Ceram Soc Bull. 1986, 65(10): 1386-1389.

[30]. Nishizaki M, Komasa S, Taguchi Y, et al. Bioactivity of NANOZR induced by alkali treatment. Int J Mol Sci. 2017, 18(4): 780.

[31]. Nawa M, Nakamoto S, Sekino T, et al. Tough and Strong Ce-TZP / Alumina Nanocomposites Doped with Titania. Ceram Int. 1998, 24(7): 497-506.

[32]. Sudo H, Kodama H A, Amagai Y， et al. In vitro differentiation and calcification in a new clonal osteogenic cell line derived from newborn mouse calvaria. J Cell Biol. 1983, 96(1): 191-198.

[33]. Liu Q, Cen L, Yin S, et al. A comparative study of proliferation and osteogenic

differentiation of adipose-derived stem cells on akermanite and β-TCP ceramics. Biomaterials. 2008, 29(36): 4792-4799.

[34]. Zigmond SH. Signal transduction and actin filament organization. Curr Opin Cell Biol. 1996, 8(1): 66-73.

[35]. Mansouri R, Hay E, Marie P J, et al. Role of syndecan-2 in osteoblast biology and pathology. BoneKEy reports, 2015, 4.

[36]. Bass M D, Morgan M R, Humphries M J. Integrins and syndecan-4 make distinct, but critical, contributions to adhesion contact formation. Soft Matter. 2007, 3(3): 372-376.

[37]. Rottner K, Faix J, Bogdan S, et al. Actin assembly mechanisms at a glance. J Cell Sci. 2017, 130(20): 3427-3435.

[38]. Kohal R J, Weng D, Bächle M, et al. Loaded custom-made zirconia and titanium implants show similar osseointegration: an animal experiment. J Periodontol. 2004, 75(9): 1262-1268.

[39]. Couchman J R. Syndecans: proteoglycan regulators of cell - surface microdomains? Nat Rev Mol Cell Bio. 2003, 4(12), 926-938.

[40]. Chen Y, Zhu J, Lum P Y, et al. Variations in DNA elucidate molecular networks that cause disease. Nature. 2008, 452(7186): 429-435.

[41]. Takeda K, Shimozono R, Noguchi T, et al. Apoptosis signal-regulating kinase (ASK) 2 functions as a mitogen-activated protein kinase kinase kinase in a heteromeric complex

with ASK1. J Biol Chem. 2007, 282(10): 7522-7531.

Tables and Figures

Table 1 Primer sequences used in qRT-PCR

Gene	Primers
Syndecan-1	F 5′ AAC CAA ATC TGG ACG GCA AA
	R 5′ CTA CTT ACG GGC CGC CAA A
Syndecan-2	F 5′ TGT AGG ACC AGA CCA AGA AAA CAG
	R 5′ TTC TCT GGC GCC TGC TCT AG
Syndecan-3	F 5′ CGT AGG CCA CTG TCA TTG TCA
	R 5′ TGG TTA GAG GAG CCA GAT GCA
Syndecan-4	F 5′ CTT CCT CCA GGC GCT CTA GA
	R 5′ CAC GTA GTC TGA AGT GAA CCG AGT T
GAPDH	F 5′ GGT GAA GGT CGG TGT GAA CG
	R 5′ CTC GCT CCT GGA AGA TGG TG

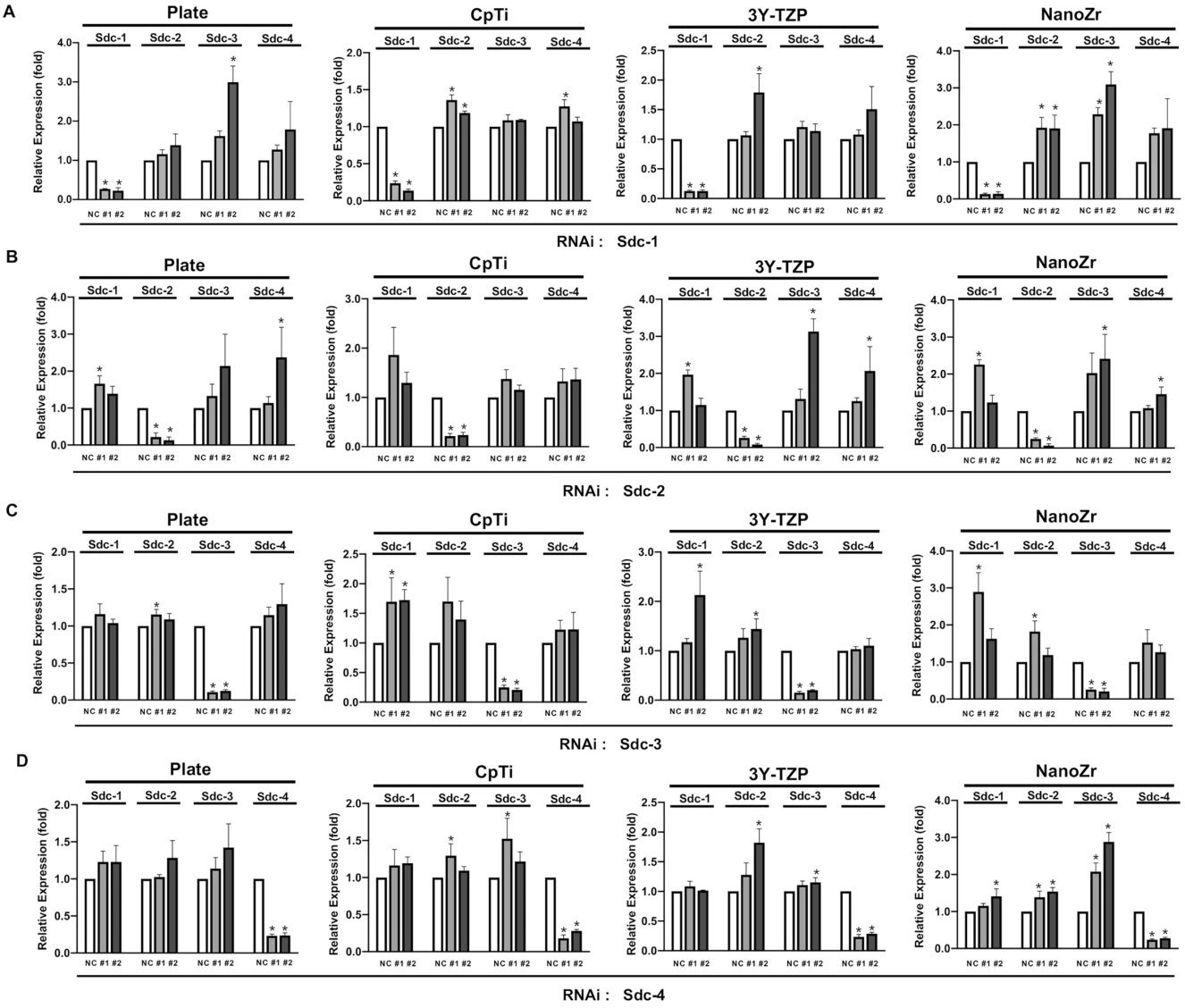

Figure 1. The expression level of Syndecan of MC3T3-E1 cells on four different surfaces (Plate, CpTi, 3Y-TZP and NanoZr) at 48h post RNAi.

Notes: MC3T3-E1 cells were transfected with a Negative Control siRNA or with siRNA that targets Syndecan-1 (#1, #2), Syndecan-2 (#1, #2), Syndecan-3 (#1, #2) and Syndecan-4 (#1, #2). Two different sequences of each of Syndecan were used respectively. (A) The expression level of Syndecans after transfected with si-Sdc1 (#1 and #2). (B) The expression level of Syndecans after transfected with si-Sdc2 (#1 and #2). (C) The expression level of Syndecans after transfected with si-Sdc3 (#1 and #2). (D) The expression level of Syndecans after transfected with si-Sdc4 (#1 and #2). The results shown are the means of three independent experiments. * A statistical significant compared to the Negative Control group ($p < 0.05$, one-way ANOVA).

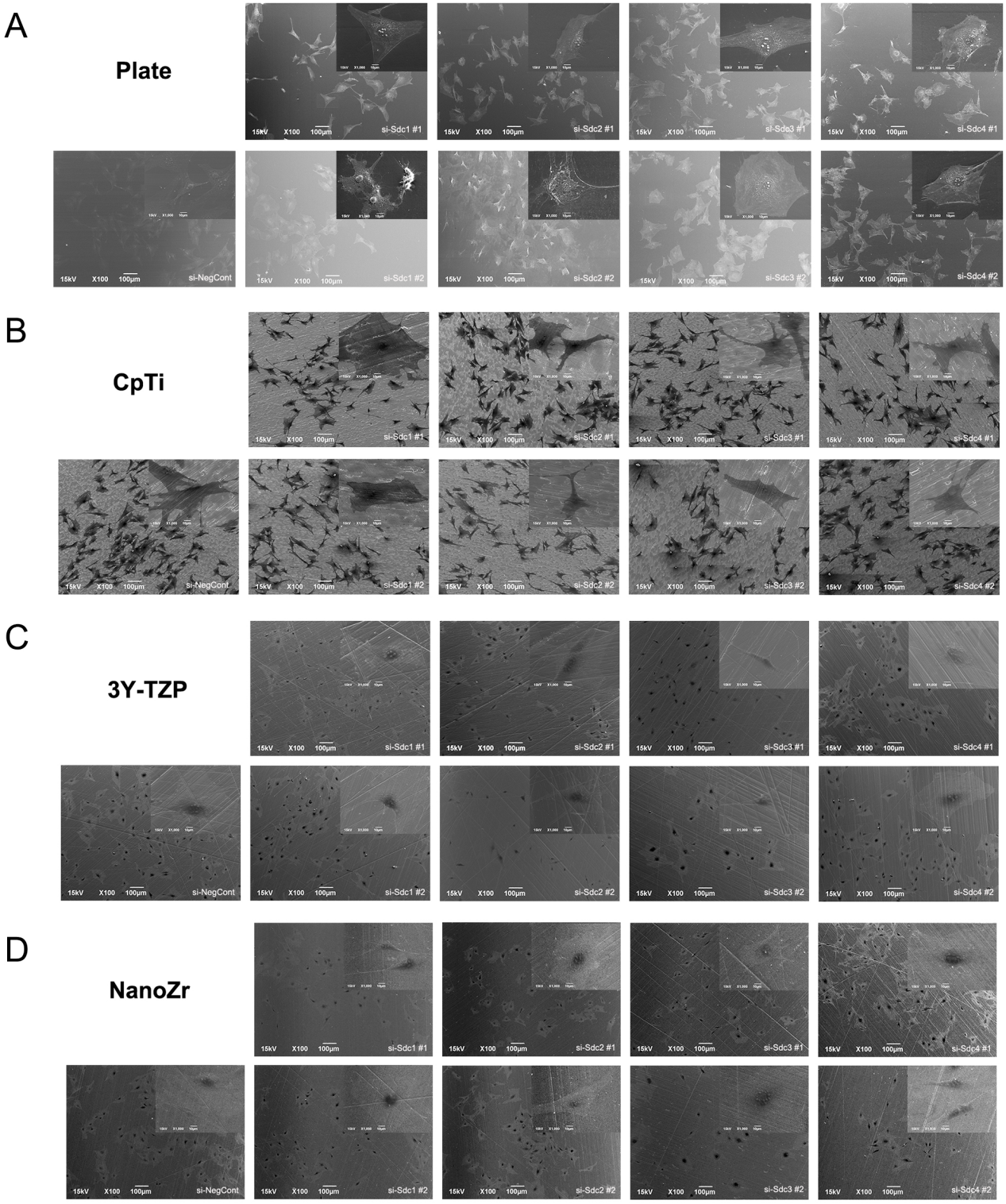

Figure 2. SEM observation of cell morphology of MC3T3-E1 cells cultured on different surfaces after 48h RNA interference treatment.

Notes: (A) Plate; (B) CpTi; (C) 3Y-TZP; (D) NanoZr. MC3T3-E1 cells were transfected with a Negative Control siRNA or with siRNA that targets Syndecan-1 (#1, #2), Syndecan-2 (#1, #2), Syndecan-3 (#1, #2) and Syndecan-4 (#1, #2). Two different sequences of each of Syndecan were used respectively. Magnification: 100x and 1000x.

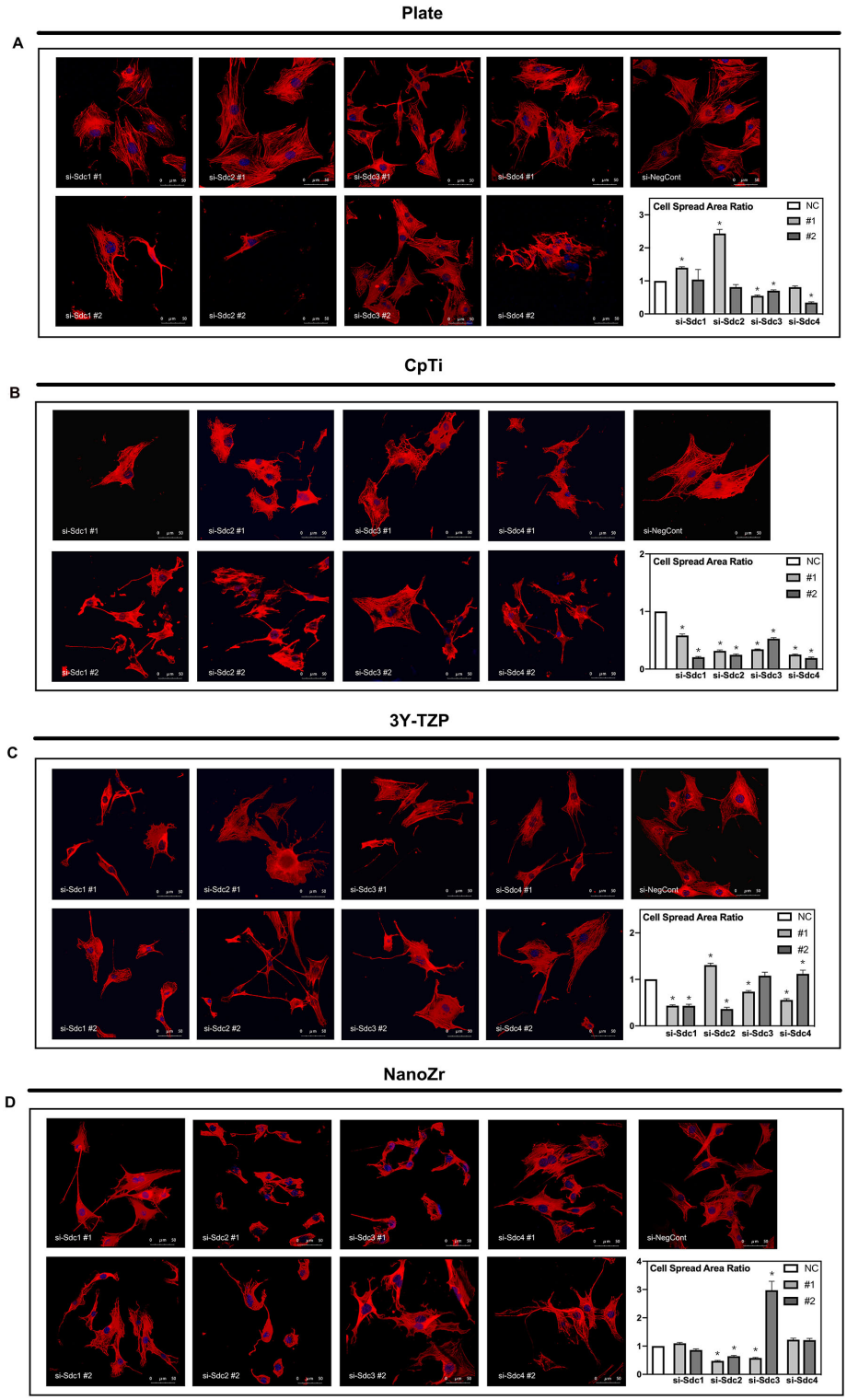

Figure 3. Observation of actin cytoskeleton and nucleus of MC3T3-E1 cells cultured on different material surfaces after 48h RNA interference treatment.

Notes: (A) Plate; (B) CpTi; (C) 3Y-TZP; (D) NanoZr. MC3T3-E1 cells were transfected with a Negative Control siRNA or with siRNA that targets Syndecan-1 (#1, #2), Syndecan-2 (#1, #2), Syndecan-3 (#1, #2) and Syndecan-4 (#1, #2). Two different sequences of each of Syndecan were used respectively. Magnification: 400x. The graph shows the MC3T3-E1 cell spread area ratio between si-Sdc group and si-NegCont group. * A statistical significant compared to the Negative Control group ($p < 0.05$, one-way ANOVA).

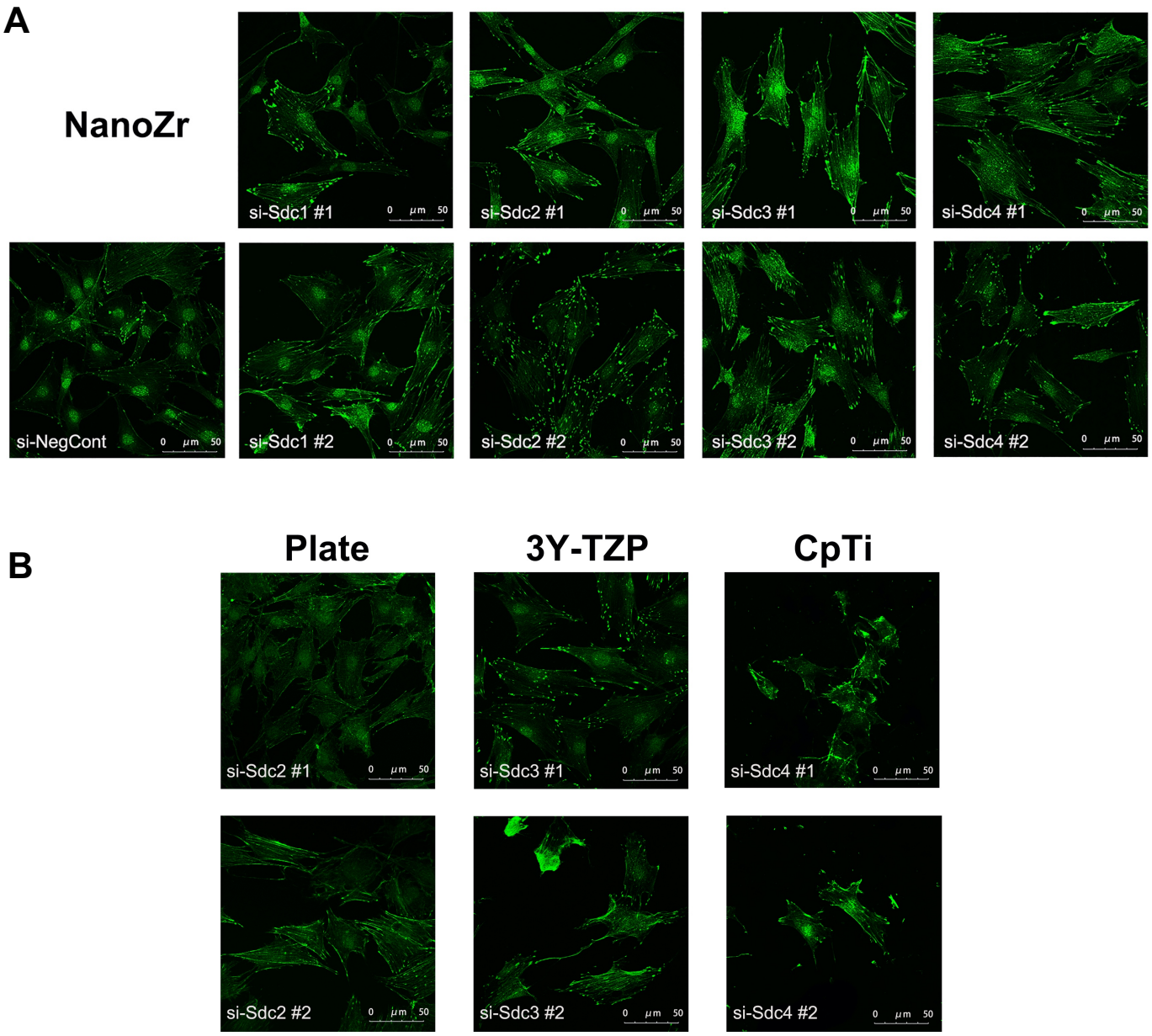

Figure 4. Organization of actin stress fibers and focal adhesion of MC3T3-E1 cells cultured on different material surfaces after 48h RNA interference treatment.

Notes: (A) NanoZr; (B) Plate, 3Y-TZP, CpTi. MC3T3-E1 cells were transfected with a Negative Control siRNA or with siRNA that targets Syndecan-1 (#1, #2), Syndecan-2 (#1, #2), Syndecan-3 (#1, #2) and Syndecan-4 (#1, #2). Two different sequences of each of Syndecan were used respectively. Magnification: 400x.

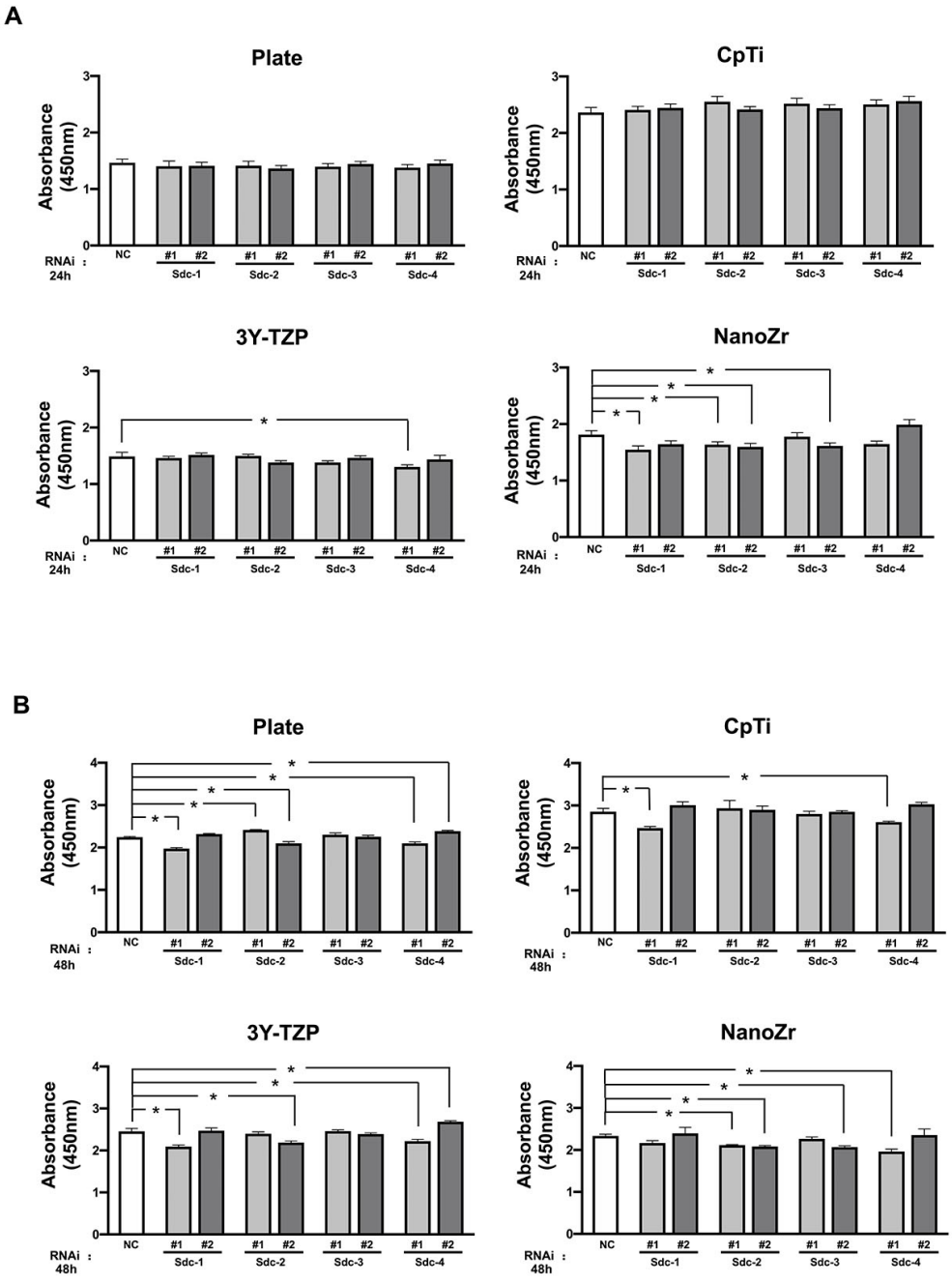

Figure 5. Cell proliferation of MC3T3-E1 cells cultured on different material surfaces (Plate, CpTi, 3Y-TZP and NanoZr) after RNAi.

Notes: MC3T3-E1 cells were transfected with a Negative Control siRNA or with siRNA that targets Syndecan-1 (#1, #2), Syndecan-2 (#1, #2), Syndecan-3 (#1, #2) and Syndecan-4 (#1, #2). Two different sequences of each of Syndecan were used respectively. (A) Absorbance value at 24h post RNAi; (B) absorbance value at 48h post RNAi. The result shows the means of three independent experiments. * A statistical significant compared to the Negative Control group ($p < 0.05$, one-way ANOVA).

Acknowledgments

My deepest gratitude goes first and foremost to Prof. Keiichi SASAKI, my supervisor, for his constant encouragement and guidance. I have been fortunate to have him as my supervisor since he provided me enough freedom and resource to conduct the research that I feel interested in. This thesis would have never been completed without the continuous support and guidance from him.

Second, I would like to express my heartfelt gratitude to Prof. Guang HONG and Hiroyuki MATSUI sensei, who has walked me through all the stages of the writing of this thesis. Without their consistent and illuminating instruction, this thesis could not have reached its present form. I am also very grateful to Taichi TENKUMO sensei for his kindness help of my experiment.

Last, my thanks would go to my beloved parents for their loving considerations, great confidence, and strong support in me all through these years. I also owe my sincere gratitude to my fellow friends who gave me their help and time in listening to me and helping me work out my problems during my oversea study and life.